Magnetic Resonance in Medicine 42:1098–1105 (1999)

Multislice Perfusion Imaging in Human Brain Using the C-FOCI Inversion Pulse: Comparison With Hyperbolic Secant

Martin N. Yongbi,[1] Yihong Yang,[2] Joseph A. Frank,[1] and Jeff H. Duyn[1]*

Perfusion studies based on pulsed arterial spin labeling have primarily applied hyperbolic secant (HS) pulses for spin inversion. To optimize perfusion sensitivity, it is highly desirable to implement the HS pulse with the same slice width as the width of the imaging pulse. Unfortunately, this approach causes interactions between the slice profiles and manifests as residual signal from static tissue in the resultant perfusion image. This problem is currently overcome by increasing the selective HS width relative to the imaging slice width. However, this solution increases the time for the labeled blood to reach the imaging slice (transit time), causing loss of perfusion sensitivity as a result of T_1 relaxation effects. In this study, we demonstrate that the preceding problems can be largely overcome by use of the C-shaped frequency offset corrected inversion (FOCI) pulse [Ordidge et al., Magn Reson Med 1996;36:562]. The implementation of this pulse for multislice perfusion imaging on the cerebrum is presented, showing substantial improvement in slice definition in vivo compared with the HS pulse. The sharper FOCI profile is shown to reduce the physical gap (or "safety margin") between the inversion and imaging slabs, resulting in a significant increase in perfusion signal without residual contamination from static tissue. The mean ± SE (n = 6) gray matter perfusion-weighted signal ($\Delta M/M_o$) without the application of vascular signal suppression gradients were 1.19 ± 0.10% (HS-flow-sensitive alternating inversion recovery [FAIR]), and 1.51 ± 0.11% for the FOCI-FAIR sequence. The corresponding values with vascular signal suppression were 0.64 ± 0.14%, and 0.91 ± 0.08% using the HS- and FOCI-FAIR sequences, respectively. Compared with the HS-based data, the FOCI-FAIR results correspond to an average increase in perfusion signal of up to between 26%–30%. Magn Reson Med 42:1098–1105, 1999. © **1999 Wiley-Liss, Inc.**

Key words: FAIR; FOCI; hyperbolic secant; perfusion

Measurement of tissue perfusion by continuous- (1–6) and pulsed-arterial spin-tagging (PAST) (7–15) methods depend on estimating very small (~1%) signal differences between a control- and a perfusion-weighted image. One of these methods, the flow-sensitive alternating inversion recovery (FAIR) (8–11), employs the difference between slice-selective and nonselective inversion-recovery (IR) images. To date, perfusion studies using FAIR or other PAST methods such as EPISTAR (7), UNFAIR (12,13), and QUIPPS (14) have utilized the hyperbolic secant (HS) pulse (16) for spin inversion. These techniques are generally characterized by low signal-to-noise ratios (SNR), which render them highly susceptible to errors caused by small signal contributions from static tissue. Additionally, the low perfusion signal necessitates long measurement times for signal averaging to achieve acceptable SNR.

For cerebral blood flow studies in humans, a major source of signal loss with FAIR or other PAST techniques (7–15) is the T_1 relaxation of the tagged blood in transit to the imaging slice. Typically the transit delay is approximately 800 msec for gray matter (15). The signal loss caused by transit delay can be reduced by improving the sharpness of the inversion pulse. This improvement will, in turn, reduce the physical gap (or safety margin) between the boundaries of the selective inversion pulse and the boundaries of the imaging slice. However, attempting to reduce the safety margin while using standard HS pulses results in slice profile interactions (Fig. 1a), which leads to residual signal from static tissue (subtraction error). To avoid the latter problem, the width of the selective HS slab is typically scaled up by a factor of about 3 compared with that of the imaging slab (7–15). Recent work from our group has shown that signal losses resulting from scaling the HS slice width can be >20% for a typical multislice FAIR study with a 50 mm imaging width (15).

In this study, we sought to minimize the static signal subtraction errors while simultaneously improving perfusion sensitivity by applying a FOCI pulse (17–20). Recently demonstrated for localized spectroscopy (19,20), FOCI pulses are a modification of the standard hyperbolic secant design in which the instantaneous offset frequency and gradient amplitude are scaled by a modulation function, *A(t)* (19,20). This scaling enables the maximum gradient amplitude to be used without requiring a corresponding increase in the peak RF amplitude. Therefore, for a given peak coil voltage, pulse bandwidth (BW) and duration, the resulting inversion profile can be up to an order of magnitude sharper than that for a standard HS. We have recently demonstrated the feasibility of applying the C-shaped FOCI RF (henceforth called FOCI RF) and gradient waveforms for *single-slice* FAIR perfusion imaging on rat brains at high field (21). Although significant minimization of subtraction errors was demonstrated, an increase in perfusion-weighted image (PWI) SNR was not observed, which was attributed to relatively long T_1 of blood at 4 T and to the high flow in rats 100 ml/100 g/min). This situation is different in humans, because cerebral blood flow rates are lower by a factor of about 2 (i.e., ~60 ml/100 g/min) (1–5), which increases transit times and decreases the perfusion SNR. These SNR losses in humans are further compounded by the fact that clinical studies are generally performed at lower field strength (1.5 T), for which the T_1 of blood is

[1]Laboratory of Diagnostic Radiology Research, National Institutes of Health, Bethesda, Maryland.

[2]Functional Neuroimaging Laboratory, Department of Psychiatry, Cornell University Medical College, New York, New York.

*Correspondence to: Jeff Duyn, Laboratory of Diagnostic Radiology Research, Building 10, Room B1N256, National Institutes of Health, 9000 Rockville Pike, Bethesda, MD 20892. E-mail: jhd@helix.nih.gov

Received 26 March 1999; revised 29 June, 1999; accepted 29 July 1999.

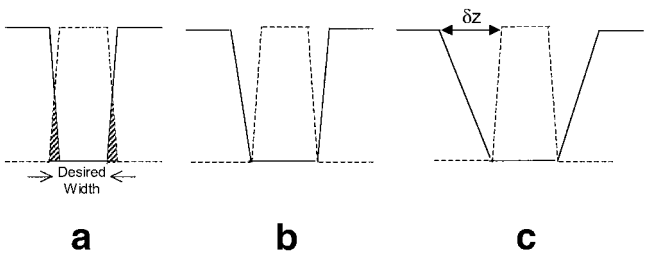

FIG. 1. (**a**) Interaction (shaded region) between the inversion- (solid line) and imaging profiles (dashed line) in a slice-selective FAIR acquisition, contributing to subtraction errors. Current approach to preventing interaction between the two profiles is to widen the useful HS slab width by either increasing the HS BW (**b**), or by reducing the selective gradient amplitude (**c**). The former has the advantage of minimizing the transition ramps (δz) but may be limited by RF power limits. However, the latter implementation is generally used as it provides more flexibility. Regardless, the increased selective inversion width increases δz and hence the time for the tagged blood to reach the imaging slice.

shorter. The shorter T_1 value causes the perfusion tag to decay faster and further decreases the perfusion sensitivity.

As already indicated, transit time losses increase with increasing selective HS widths and the width of its slice profile ramps. The widths of the ramps (δz) increase as the selective HS gradient decreases, i.e., $\delta z \propto 1/G_{sel}$. For a constant BW, G_{sel} is inversely proportionate to the width of the selective HS slab and δz. For multislice FAIR imaging covering 10 or more slices, selective HS slabs widths of ≥100 mm are normally required for flow weighted acquisitions (15). Such large slabs result in relatively wider HS ramps, due to the low gradient amplitudes (~1 mT/m) required. Smaller profile ramps are achieved using FOCI pulses, where the selection gradient amplitude is deliberately scaled up by factors of ≥5 or higher by multiplying with a modulating function *A(t)* (19,20). This scaling minimizes the widths of the ramps to enable the use of nearly the same inversion and imaging widths, without increasing the risk of interaction.

In this article, we describe the implementation and application of the FOCI pulse for multislice perfusion imaging on human brain using FAIR. The performance of the FOCI is compared with a regular HS pulse and shown to provide significant improvement in perfusion sensitivity, while simultaneously minimizing subtraction errors from static tissue. To our knowledge, this application is the first of its kind for clinical cerebral perfusion studies.

MATERIALS AND METHODS

FOCI Implementation

Amplitude [$B_1(t)$] and frequency [$\Delta\omega(t)$] waveforms for the HS pulse were generated from the Silver-Hoult equations (16):

$$B_1^{HS}(t) = \text{Sech}\,(\beta t)$$

$$\Delta\omega^{HS}(t) = -\mu\beta\,\tanh\,(\beta t). \qquad [1]$$

To ensure optimal performance, the following considerations were taken into account while designing the FOCI and HS waveforms (19):

1. Higher values of the parameter μ (16) increase the sharpness of the inversion profile but also correspond to smaller values of β (because $\beta \propto BW/\mu$). On the other hand, decreasing β in order to optimize μ will increase the width of the pulse envelope, thus increasing the risk of truncation. Hence, selecting optimal HS parameters (for given BW) required a compromise between μ and β. Generally, good HS profiles are obtained when μ≥4 (16). In this application, β and μ values of 1361 and 6 were used, respectively. When combined with a pulse length of 16.386 msec, these parameters yielded a truncation level of <0.03% of the maximum HS amplitude. This pulse is slightly longer than those used in previous studies (7–15), yet no significant degradation of the slice profile is expected because of the relatively long blood and tissue T_2 values in human brain at 1.5 T.
2. 1024 points were used to define the gradient and RF waveforms, yielding a digitization interval of only 16 μsec. This small digitization interval is important to minimize excitation side bands within the sensitive volume of the RF coil (20).
3. The C-FOCI design was selected because it has been shown to provide the sharpest profile of all the FOCI pulses (19,20). Parameters for the modulation function, *A(t)* (16), were selected based on our maximum gradient amplitude of 22 mT/m and implemented in the same manner as previously described (21). To avoid gradient overload, the following *A(t)* was used:

$$A(t) = \frac{1}{\text{Sech}\,(\beta t)} \text{ when Sech } (\beta t) > 0.095$$

$$= 10.50 \qquad \text{otherwise.} \qquad [2]$$

Other FOCI parameters (μβ BW) were identical to those used for the HS. Using a maximum value of *A(t)* ($A(t)^{max}$) value of 10.50, and coupled with our system hardware maximum gradients of 22 mT/m, the minimum FOCI slab thickness [min_sl (mm)] possible with the preceding *A(t)* was 25 mm, where

$$\text{min\_sl} = \frac{A(t)^{\max} * \text{BW}^{\text{HS}}(\text{Hz})}{\gamma * 22\text{mT/m}} \qquad [3]$$

and γ is the ^{1}H gyromagnetic ratio (42.58 MHz/T). Wider inversion slabs were possible by using smaller BWs, or by proportionately reducing the maximum scaling factor.

The FOCI FAIR Sequence

The FOCI-based FAIR sequence (Fig. 2) was similar in many respects to that proposed by Yang et al. (15), but with the following modifications: i) FOCI RF and gradient pulses were added in the first half of the sequence, Fig. 2; ii) Bipolar gradients ($\mathbf{G}_p/\mathbf{G}_n$) were implemented immediately after the slice select refocusing gradient, and on all three axes for suppressing intravascular signal. Enhanced vascular signal crushing was possible either by increasing $\mathbf{G}_p/\mathbf{G}_n$, or Δ. This implementation is more efficient than the

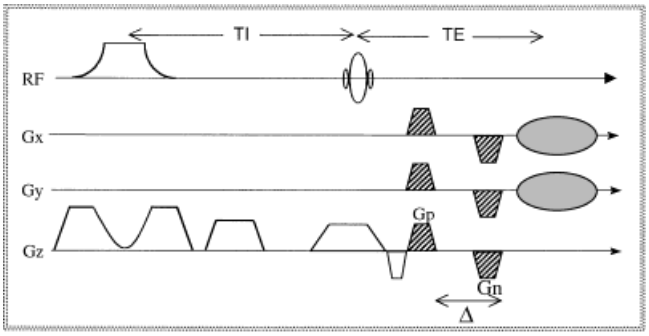

FIG. 2. Modified spiral FAIR sequence with C-shape FOCI RF and gradient waveform. Bipolar crusher gradients (hatched) with a variable Δ were implemented in all three directions. Gradient within TI period is for dephasing unwanted FID created by the inversion pulse. Readout pulse was five lobe, 4 msec hamming filtered sinc.

previous design (14) since it allows for the same crusher intensity at a significantly reduced TE/TR. A fast single-shot spiral sequence capable of a minimum acquisition time of 22 msec was used for signal readout. This short readout time allowed the acquisition of a high number of slices (≥10) under 250 msec compared with ~1000 msec common with EPI-based multislice FAIR studies.

Studies were performed on a 1.5-T MR system (General Electric, Milwaukee, WI) using a quadrature head coil and shielded gradients with a slew rate of 120 T/m/sec. All clinical studies were performed as part of an approved Intramural Review Board Protocol at the National Institutes of Health.

The performance of the HS- and FOCI-FAIR sequences were evaluated by comparing their respective a) subtraction errors; b) vascular signal contribution; c) inversion profiles in human brain; and d) SNR in perfusion imaging.

Subtraction Errors

Phantom and human brain studies were performed to assess subtraction errors when either the FOCI or HS inversion was applied. The phantom consisted of a 15 cm (internal diameter) agar gel phantom with T_1/T_2~900/90 msec, consistent with human brain gray matter at 1.5 T. The subtraction errors using this phantom were evaluated by using the following protocol: Using a nonselective HS pulse, inversion-recovery (IR) images (ten 5-mm-thick slices) were acquired followed by a corresponding multislice set of HS selective IR images. The width of the inverted slab for the selective HS was initially set to 50 mm so as to encompass the entire ten 5-mm slices. The selective HS width was progressively increased (up to 150 mm), and the entire procedure repeated for each individual HS width. Subtraction errors were calculated using the signal difference between the nonselective IR and selective IR images. The above procedure was repeated with the FOCI pulse. Other parameters were as follows: relaxation delay, 3 sec; readout-time, 35 msec; TE, 8 msec; inversion delay (TI), 1200 msec (first slice); field of view (FOV), 240 mm; and NEX, 5, where NEX denotes the averaged number of difference images obtained from selective and nonselective IR pairs. All measurements were preceded by six prescans to allow the magnetization to reach equilibrium.

The above calibration protocol for subtraction error was evaluated using a healthy volunteer. To eliminate the perfusion signal caused by blood flow, the subject was administered a double dose of gadopentetate dimeglumine (Gd-DTPA) (single dose, 0.1 mmol/kg). The Gd-DTPA administration results in negligible perfusion signal because the T_1 of blood is reduced from ~1200 msec to 300 msec, which causes the rapid relaxation of the arterial tag during the transit time. Multislice FAIR images (ten 5-mm slices) were acquired pre– and post–Gd-DTPA administration. The minimum selective inversion widths for the FOCI and HS corresponded to the widths used in the experiments with the phantom that indicated no residual subtraction error. Other parameters were identical to those used above, except that NEX was set to 20 in order to obtain acceptable PWI SNR.

FOCI and HS B1 Calibration

Threshold voltages required for the inversion pulses were established by acquiring a series of multislice (10) human brain FAIR (ΔM) images over a range of RF power settings. This accounts for possible spatial variations in the threshold RF amplitude, which may arise due to nonuniform B1 field effects. This approach is particularly important along the long-axis of the head-coil in order to minimize in-flow of untagged arterial spins (coil in-flow) during the TI period. The measurement parameters were identical to those used in the previous section.

Vascular Crusher Gradient Calibration

The contribution of intravascular signal on the FAIR signal has already been examined in studies employing HS inversion (15). It was necessary to repeat this study to compare and contrast previous results with those obtained using the FOCI pulse. A series of multislice ΔM images were obtained with increasing crusher gradient intensity (or *b*-values) in which the separation (Δ) between the crusher gradients (Fig. 2) was progressively increased while maintaining the bipolar gradient amplitudes at maximum. The FOCI and HS slab widths were 80 mm and 120 mm, respectively, to avoid interaction between the imaging and inversion profiles (see subtraction error results).

Slice Profiles

Among other factors, the quality (sharpness) of the inversion depends on the degree of magnetic susceptibility, relaxation effects, and flow. In view of the differences in magnetic susceptibility, relaxation times, blood flow in the brain, and water phantoms, RF profile evaluations should *ideally* be performed in vivo. Therefore, to determine the quality of the inversion for the two pulses, a slab in the brain was inverted orthogonal to the imaging plane. A FLASH imaging technique was used to acquire high-resolution (256 × 256) images. The high-resolution minimizes Gibbs ringing that may adversely affect the evaluation of the transition zones at the edges of the inversion profiles. To ensure inversion, the RF transmitter power setting was set 50% above the threshold value determined, in vivo, in an earlier study. In order to allow clear visualization of the selected inversion band, it was desired

to select an inversion delay to null the signal from the band. While the latter is easily achievable in homogenous samples (e.g. phantoms), this is not possible in human brain that consist of several tissue types (gray matter, white matter, cerebrospinal fluid) with a range of T_1 between ~500 msec to ~2500 msec at 1.5 T. Images were therefore acquired using a range of TI values (300–1000 msec) to cover gray and white matter null points. Other measurement parameters were as fllows: FOV, 24 cm; TR, 2 sec; number of acquisitions, 1.

Perfusion-Weighted Imaging

To compare the relative performance of the FOCI and HS for multislice perfusion imaging, ΔM was measured with and without suppression of vascular signal in healthy volunteer brain (n = 6). Measurement parameters for perfusion-weighted imaging were as follows: relaxation delay, 2.5 sec; readout time, 42 msec; TE, 15 msec; TI, 1200 msec (first slice); number of slices, 10; slice thickness, 5 mm; FOV, 240 mm; NEX, 20. FOCI and HS slab widths were 80 mm and 120 mm, respectively.

Inversion recovery images (for T_1 map calculation) were acquired with the FAIR sequence using the HS pulse applied in a nonselective mode. TI values for the first slice were as follows 0.01, 0.05, 0.1, 0.3, 0.5, 0.7, 0.9, 1.1, 1.3, 1.6, 1.9, 2.2, and 2.5 sec. Other parameters were as follows: TE, 15 msec; readout time, 42 msec; relaxation delay, 8 sec; and number of acquisitions, 10. T_1 maps (calculated from a three-parameter fit to the IR data) were used for segmenting ΔM images into gray and white matter regions of interest (ROI). Voxels with T_1 values between 500–700 msec were assigned to white matter, while voxels with T_1 values in the range of 900–1100 msec were assigned to gray matter.

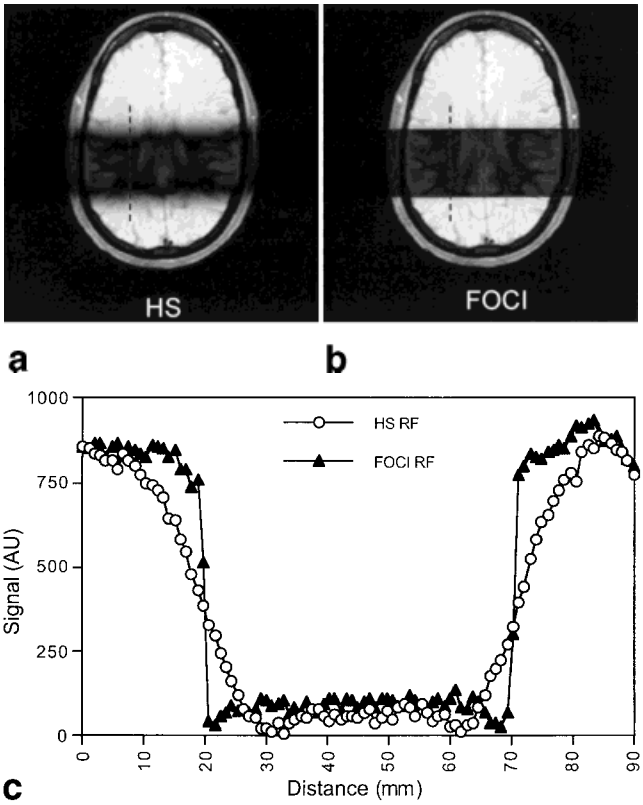

FIG. 3. Demonstration of the relative slice-profile performance of the HS and FOCI pulses on human brain: (**a**) HS and (**b**) FOCI inversion bands obtained with a standard gradient-echo sequence on volunteer brain. The high selectivity of the FOCI pulse is clearly reflected by excellent delineation at the edges of its profiles. This is further illustrated in **c**, depicting HS and FOCI line-profile plots derived from the same spatial positions (vertical lines) in images **a** and **b**.

RESULTS AND DISCUSSION

FOCI and HS Profiles and B1 Calibration—In Vivo

An example of the quality of the FOCI and HS inversion band (width, 50 mm) acquired in a healthy subject are shown in Fig. 3a and b. The FOCI pulse showed substantially better edge definition, Fig. 3b. This improvement further demonstrated in Fig. 3c, which is a plot of the FOCI and HS line-profiles obtained from the same spatial location in the images shown in Fig. 3a and b. The apparent lack of complete inversion at the center of the profiles is due to the fact that these images were acquired with a TI of 300 msec to null the signal within the RF BW in order to visualize the inversion band. This is clearly difficult in human brain due to the range of T_1 values combined with partial volume effects, hence the slight regrowth of z-magnetization at the center of the profiles. Excellent delineation at the edges of the FOCI band is reflected in its relatively narrow transition zones (ramps), where spins are neither fully relaxed nor inverted.

The B1 calibration results (not shown) obtained on the brain of a volunteer showed no significant difference between the required inversion threshold voltages between the FOCI and HS pulses, and also confirmed the adiabatic behavior of the pulses. The latter finding is not surprising since identical parameters (BW, μ, and pulse lengths) were used to design both RF pulses. A similar finding based on a phantom study was recently reported by Payne and Leach (20).

Static Signal Subtraction Errors

The residual static signal in ΔM images obtained on phantoms with the FOCI and HS FAIR sequences are shown in Fig. 4a. At a selective FOCI width of 50 mm, the ΔM images showed excellent static signal suppression, with residual intensities within the noise level in eight of the 10 slices (Fig. 4a, panel iii). On the other hand, only four of the 10 HS-FAIR images were free of subtraction errors for the same selective slab width (Fig. 4a, panel ii). As shown in Fig. 4a, panel v, the FOCI slab width required to achieve ΔM images void of subtraction errors in all 10 slices was 65 mm. This represents a fractional increase of 30% of the imaging slab width. In order to achieve similar results with the HS pulse, a slab width of at least 120 mm, representing more than 140% increase over the imaging dimension, was required.

A plot of the subtraction error as a percentage of the nonselective IR signal (averaged over all 10 phantom slices) is shown in Fig. 4b for both FOCI and HS pulses. The difference in the sharpness of the HS and FOCI profiles is reflected in the substantial difference in the subtraction error when the slab thickness was <80 mm. As expected,

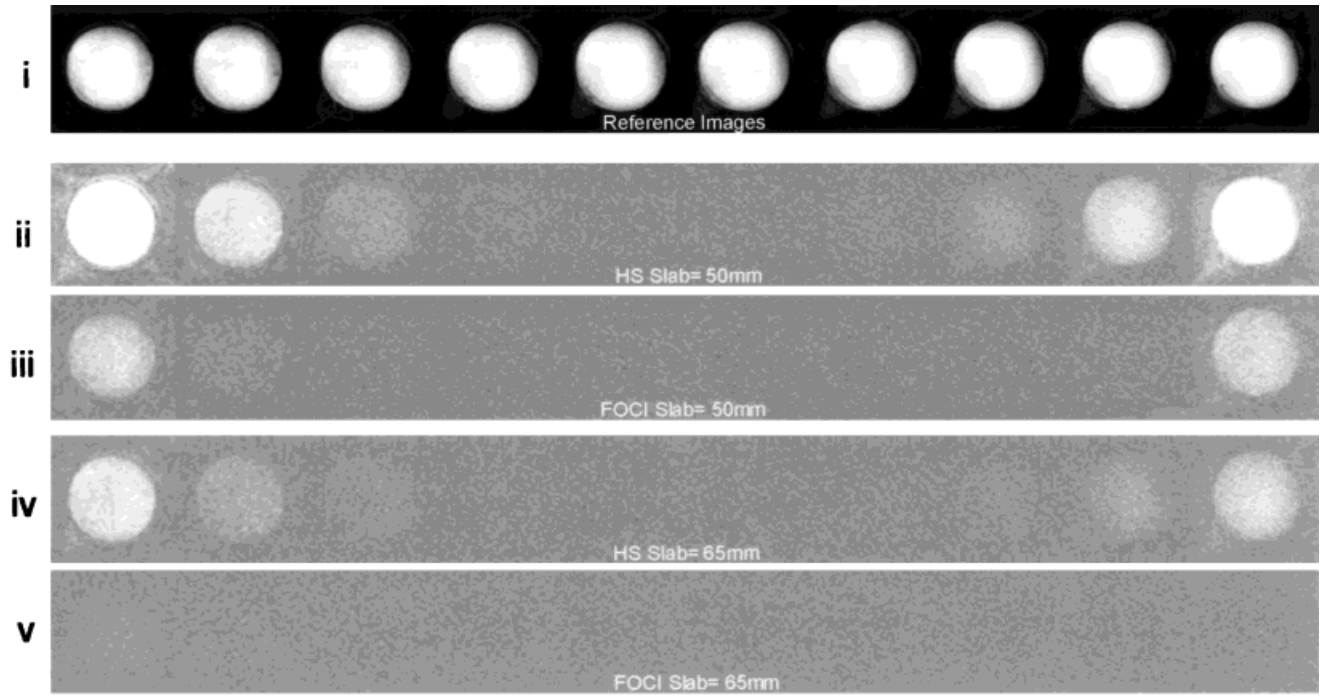

a

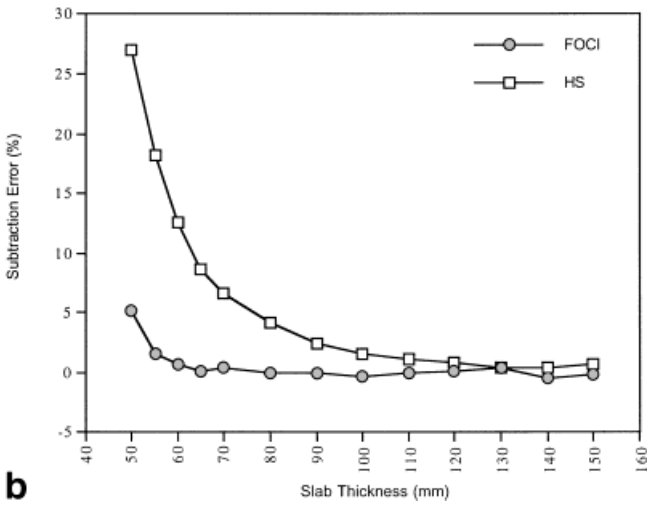

b

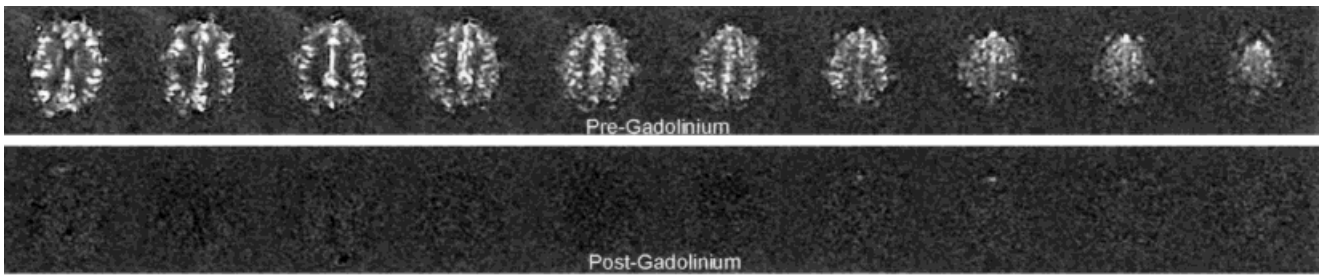

c

FIG. 4. **a:** (i) Reference phantom images, 10 slices covering a 50 imaging width; phantom subtraction images obtained with (ii) HS and (iii) FOCI selective widths of 50 mm; (iv) subtraction images acquired using HS width of 65 mm and (v) corresponding subtraction images acquired with a FOCI width of 65 mm demonstrating clean subtraction for all 10 slices. **b:** Plot of residual subtraction error versus HS and FOCI slab width. **c:** Validation of FOCI subtraction on normal human volunteer brain: FOCI-based ΔM images pre– and post–Gd-DTPA administration. Lack of residual signal in ΔM images after Gd-DTPA administration validates the calibration procedure. The HS width required to achieve identical post–Gd-DTPA subtraction images was ~130 mm.

the subtraction errors decreased with increasing slab width, indicating that slice profile interactions, not motion induced by the gradient hardware, were responsible. Once more the rate of decrease of the subtraction error with inversion slab width was much higher for the FOCI-FAIR sequence.

An example of ΔM images acquired pre and post–Gd-DTPA administration from a healthy volunteer are shown in Fig. 4c. For this study, a selective FOCI width of ≥75 mm (≥130 mm for HS) was required to reduce the static signal to noise level, as opposed to 65 mm required in the above phantom study. The required HS width was ≥130 mm.

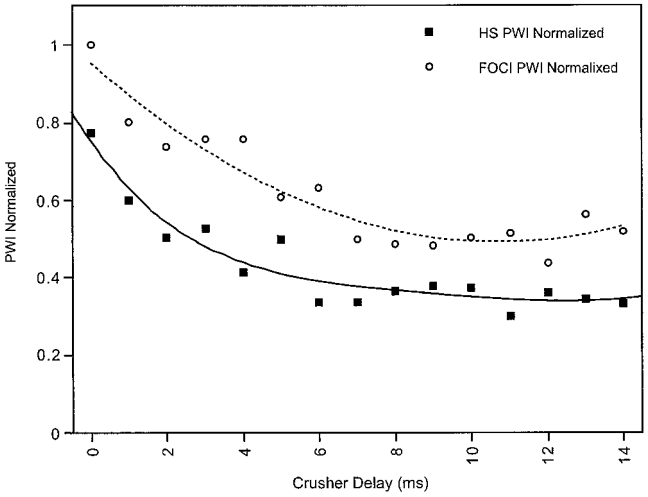

FIG. 5. Plot of ΔM versus vascular crusher gradient separation. Signal was normalized to the first data point acquired without vascular signal crushing.

This discrepancy may be caused by differences in flow and magnetic susceptibilities between brain tissue and phantom, and these effects may modulate the inversion profiles differently in the two media. This is interesting, as it highlights the need for such validation to be performed in vivo if the subtraction errors are to be completely eliminated. Extended details of the latter protocol will be outlined in another communication.

The differences in subtraction errors observed for the FOCI and HS based FAIR sequences are caused by differences in their inversion profiles. The more rectangular FOCI profile allows the use of thinner selective inversion slabs in the FAIR studies. Similar findings were recently reported by Pell et al. (23) in which the inversion efficiency of both pulses was evaluated. The reduced ramps and selective slab width of the FOCI pulse can be expected to combine to reduce the transit time of arterial blood, hence increasing the perfusion SNR. The required HS width in this study is significantly larger than that reported in a recent related study by Yang et al. (15). The fact that a clean subtraction was not obtained in all 10 slices in the preceding study partly accounts for this discrepancy. Another factor may be due to differences in HS BW in the study by Yang et al. (15) (~3000 Hz) and that used in this work (2600 Hz). Higher HS bandwidths generally require higher RF power for inversion resulting in more RF power deposition. In this study, both the HS and FOCI bandwidths were selected to be in the range of values generally used for clinical imaging (2000–3000 Hz). Therefore relatively lower subtraction errors compared with those obtained in this study may be expected for an HS pulse of a higher bandwidth.

Effect of Vascular Crusher Gradient

Figure 5 shows the dependence of the total ΔM signal, integrated over all 10 slices, on the crusher gradient separation, Δ. In both cases, increasing the crusher gradient intensity progressively decreased ΔM which reached a plateau at a Δ of around 7 msec (b−value~4 sec/mm^2). The average ΔM remained relatively constant above this Δ value, suggesting that signal from the arterial vessels has been substantially eliminated (6,15). Consistent with previous studies (6,15), a total decrease in ΔM of about 50% was observed for both the HS- and FOCI-FAIR sequences.

FOCI and HS Multislice FAIR Data

An example of ΔM images acquired from one volunteer using identical measurement parameters are shown in Fig. 6a. The qualitative differences between the FOCI and HS sequences as reflected by the differences in contrast and signal intensity is readily apparent. These differences are more pronounced in the superior slices, which is attributed to the higher transit times of these slices in view of the significant differences in the required HS and FOCI slab

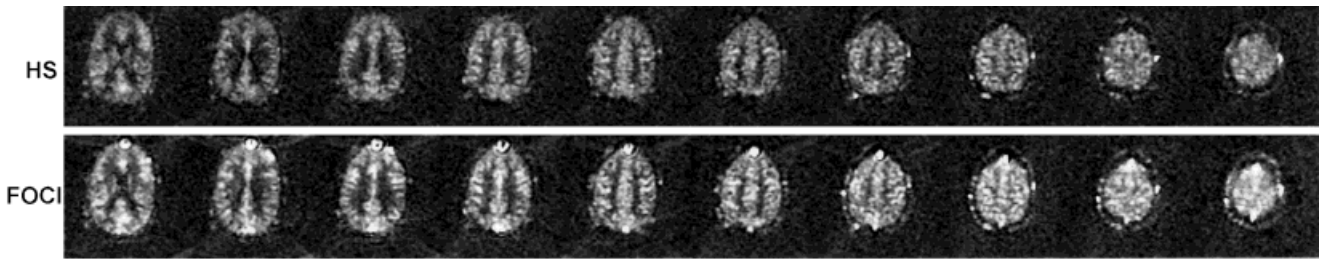

a

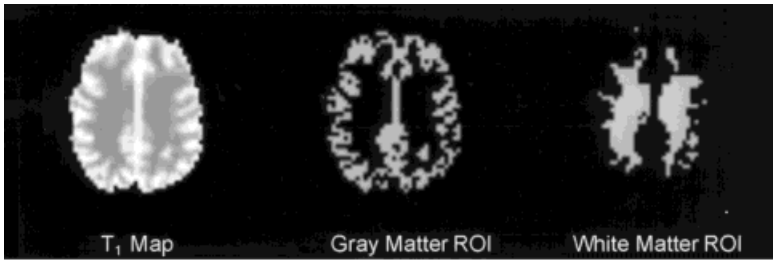

b

FIG. 6. **a:** Multislice FAIR images acquired with HS- and FOCI-FAIR sequence. The FOCI-based images manifest an overall better signal and contrast. **b:** Demonstration of gray-white matter segmentation using calculated T_1 maps.

widths. Areas of intense localized vascular signals are apparent on these images. This high vascular contribution is primarily caused by using relatively short TI delay (TI, 1.2 sec), with no crusher gradients. The vascular signal contributions were consistently more pronounced in the FOCI-based acquisitions. The latter observation is once more attributed to the shorter transit time and reduced saturation effects on the in-flowing arterial blood at the edges of the FOCI profile. Overall, the FOCI-based FAIR images consistently provide better overall perfusion signal.

A quantitative comparison of gray matter ΔM obtained with the FOCI and HS sequences was performed using segmentation maps generated from the calculated T_1 maps. An example of gray/white matter ROI segmentation is shown in Fig. 6b. In view of the relatively low resolution of the T_1 weighted IR images (64 × 64), some degree of partial volume contamination was unavoidable. The segmentation analysis was restricted to the first six slices (inferior to superior) which allowed for better gray/white matter segmentation.

A plot of the average $\Delta M/M_o$ in gray matter against slice number is shown in Fig. 7a and b. In these graphs, slice number increase distally from inferior to superior. The mean $\Delta M/M_o$ (± SE) for the HS-FAIR sequence without vascular crushers ranged from 1.07 ± 0.13 % (slice 6) to 1.78 ± 0.02 % (slice 1) (Fig. 7a). The corresponding range for the FOCI FAIR sequence was from 1.43 ± 0.15 % (slice 6) to 1.80 ± 0.05 % (slice 1). The ΔM signal decreased with increasing slice number for both HS and FOCI sequences. The decline in ΔM with increasing slice number is due to an increase in the transit time as you move distally, coupled with the fact that the acquisition order of the slices was superior to inferior. A similar trend was also manifested in the HS and FOCI-based FAIR ΔM signal acquired with the application of vascular signal suppression gradients (Fig. 7b). The mean $\Delta M/M_o$ (± SE) without vascular signal suppression, integrated over all the six slices was 1.19 ± 0.10% for the HS-based FAIR, and 1.51 ± 0.11% for the FOCI-based sequence. The corresponding values with vascular signal suppression were 0.64 ± 0.14 % for the HS-FAIR, and 0.91 ± 0.08% for the FOCI-based FAIR sequence. These results (Fig. 7c) represent ΔM signal increase of between 26% to 30% (without and with crushers) for the FOCI-based data over the corresponding HS-FAIR results.

In a previous study, no such improvement in ΔM was shown when the FOCI pulse was used instead of the HS pulse for perfusion imaging in rat brain at 4 T (21). The difference between our results and the latter study can be attributed to the difference in T_1 values between arterial blood T_1 at 1.5 T (~1.2 sec) and 4 T (~1.7 sec). Additionally, the higher blood velocity in rats (by a factor of ~2) compared with humans significantly decreases the arterial transit time in rats. It is also important to note that the previous animal study was based on single slice acquisitions for which the selective HS inversion profiles are relatively square, due to the smaller slab widths employed.

The above results show the advantages of applying the FOCI pulse to the HS pulses for PAST measurements of tissue perfusion. The FOCI-FAIR sequence provides significantly better perfusion sensitivity while simultaneously minimizing subtraction errors from static tissue. These

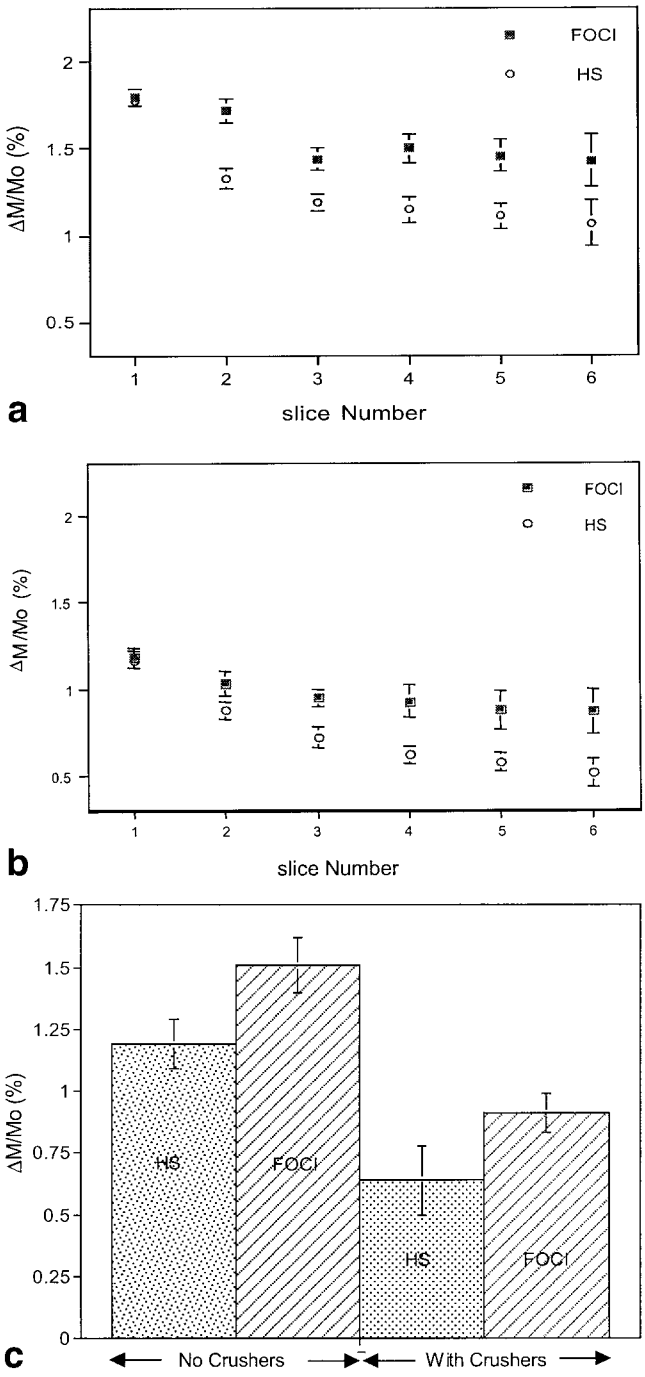

FIG. 7. Comparison of FAIR signal acquired using HS and FOCI tagging pulses: Average gray matter $\Delta M/M_o$ (n = 6) plotted against slice number. **a:** No vascular signal crushing. **b:** Corresponding plot on the same scale for data acquired with vascular crushing. Slice numbers increase distally from inferior to superior. **c:** Mean $\Delta M/M_o$ (± SE) of all six slices obtained without and with suppression of vascular signal.

advantages are primarily due to the better edge definition of the FOCI pulse which minimizes the physical gap. In fact, Wong et al. have determined experimentally that the transit delays is ~500–1500 msec for a physical gap of 1–3 cm between the tag region and the imaging slice (24). The FOCI pulse minimizes the gap by a factor of ~3, leading to

reduced arterial transit time, and results in substantial improvements in the FAIR signal.

CONCLUSION

There are significant advantages of using the FOCI inversion over conventional HS pulses for multislice FAIR perfusion imaging. The sharper FOCI profile yields perfusion-weighted images that are free of static signal subtraction errors at relatively smaller selective slab widths. The reduced FOCI width minimizes transit times and results in a significant increase in the perfusion signal. The advantages of the FOCI pulse over HS pulses will be most noticeable in humans at lower, clinically relevant field strengths due to reduced transit time losses made possible by improvement in slice profile with the FOCI pulse. Although the current FOCI demonstration is based on the FAIR technique, similar advantages apply for other pulsed arterial tagging methods such as EPISTAR, QUIPPS, and UNFAIR.

ACKNOWLEDGMENTS

The authors acknowledge helpful discussions on slice profiles and arterial transit times with Keith St. Lawrence, Ph.D. (LDRR Laboratory, National Institutes of Health) and Jody L. Tanabe, M.D. (University of Colorado Health Sciences Center). Technical assistance from Bobbi K. Lewis, B.A. (LDRR Laboratory, National Institutes of Health) is gratefully acknowledged.

REFERENCES

1. Detre JA, Leigh JS, Williams DS, Koretsky AP. Perfusion imaging. Magn Reson Med 1992;23:37–45.
2. Williams DS, Detre JA, Leigh JS, Koretsky AP. Magnetic resonance imaging of perfusion using spin inversion of arterial water. Proc Natl Acad Sci USA 1992;89:212–216.
3. Zhang D, Williams DS, Detre JA, Koretsky AP. Measurement of brain perfusion by volume-localized NMR spectroscopy using inversion of arterial water spins: accounting for transit times and cross-relaxation. Magn Reson Med 1992;25**:**362–371.
4. Roberts DA, Detre JA, Bolinger L, Insko EK, Leigh JS. Quantitative magnetic resonance imaging of human brain perfusion at 1.5 T using steady-state inversion of arterial water. Proc Natl Acad Sci USA 1994;91:33–37.
5. Zhang W, Silva A, Williams D, Koretsky A. NMR measurement of perfusion using arterial spin-labelling without saturation of macromolecules spins. Magn Reson Med 1995;33:370–376.
6. Ye FQ, Pekar JJ, Jezzard P, Duyn J, Frank JA, McLaughlin AC. Perfusion imaging of the human brain at 1.5 T using a single-short EPI spin tagging approach. Magn Reson Med 1996;36:219–224.
7. Edelman RR, Siewert B, Darby BG, Thangaraj V, Nobre AC, Mesulam MM, Warach S. Qualitative mapping of cerebral blood flow and functional localization with echo-planar MR imaging and signal targeting with alternating radio frequency. Radiology 1994;192:513–520.
8. Kwong KK, Chesler DA, Weisskoff RM, Donahue KM, Davis TL, Ostergaard L, Campbell A, Rosen BR. MR perfusion studies with T_1-weighted echo planar imaging. Magn Reson Med 1995;34:878–887.
9. Kim S-G. Quantification of relative cerebral blood flow change by flow sensitive alternating inversion recovery (FAIR) technique: application to functional mapping. Magn Reson Med 1995;34:293–301.
10. Schwarzbauer C, Morrisey S, Haase A. Quantitative magnetic resonance imaging of perfusion using magnetic labeling of water proton spins within the detection slice. Magn Reson Med 1996;35:540–546.
11. Kim S-G, Tsekos NV. Perfusion imaging by a flow-sensitive alternating inversion recovery (FAIR) technique: application to functional brain imaging. Magn Reson Med 1997;37:425–435.
12. Helpern JA, Branch CA, Yongbi MN, Huang NC. Perfusion imaging by un-inverted flow-sensitive alternating inversion recovery (UNFAIR). Magn Reson Imaging 1997;15:135–139.
13. Tanabe JL, Yongbi M, Branch CA, Hrabe J, Johnson G, Helpern JA. MR perfusion imaging in human brain using the UNFAIR technique. J Magn Reson Imaging 1999;9:761–767.
14. Wong EC, Buxton RB, Frank LR. Quantitative imaging of perfusion using a single subtraction (QUIPSS and QUIPPS II). Magn Reson Med 1998;39:702–708.
15. Yang Y, Frank JA, Hou L, Ye FQ, McLaughlin AC, Duyn JH. Multislice imaging of quantitative cerebral perfusion with pulsed arterial spin labeling. Magn Reson Med 1998;39:825–832.
16. Silver MS, Joseph RI, Hoult DI. Selective spin inversion in nuclear magnetic resonance and coherence optics through an exact solution of the Bloch-Riccati equations. Phys Rev 1985;A31:2753–2755.
17. Connoly S, Nishimura D, Macovski A. Variable rate selective excitation. J Magn Reson 1988;78:440–458.
18. Matson FB. FOCI pulses re-visited as re-mapped hyperbolic secant pulses tagging with the FOCI pulse. In: Proceedings of the ISMRM 7th Scientific Meeting, Philadelphia, PA, 1999. p 2086.
19. Ordidge RJ, Wylezinska M, Hugg JW, Biutterworth E, Franconi F. Frequency offset corrected inversion (FOCI) pulses for use in localized spectroscopy. Magn Reson Med 1996;36:562–566.
20. Payne GS, Leach MO. Implementation and evaluation of frequency offset corrected inversion (FOCI) pulses on a clinical MR system. Magn Reson Med 1997;38:828.
21. Yongbi, MN, Branch CA, Helpern JA. Perfusion imaging using FOCI RF pulses. Magn Reson Med 1998;40:938–943.
22. Wong EC, Buxton RB, Frank LR. A theoretical and experimental comparison of continuous and pulsed arterial spin labeling techniques for quantitative perfusion imaging. Magn Reson Med 1998 40:348–355.
23. Pell GS, Thomas DL, Lythgoe MF, Calamante FC, Howseman AM, Williams SR, Gadian DG, Ordidge RJ. Measurement of perfusion using arterial spin-tagging with the FOCI pulse. In: Proceedings of ISMRM 6th Scientific Meeting, Sydney, Australia, 1998. p 1190.
24. Wong EC, Buxton RB, Frank LR. Implementation of quantitative perfusion imaging techniques for functional brain mapping using pulsed arterial spin labeling. NMR Biomed 1997;10:237–249.